The Gram-positive model organism *Bacillus subtilis* does not form detectable cardiolipin-specific lipid domains

Authors: Alex-Rose Pogmore, Kenneth H. Seistrup, and Henrik Strahl

Author affiliation: Centre for Bacterial Cell Biology, Institute for Cell and Molecular Biosciences, Newcastle University, Newcastle upon Tyne, United Kingdom

Correspondence: Henrik Strahl, email: h.strahl@ncl.ac.uk, tel: +44 (0) 191 208 3240

Keywords: Lipid domains, Phospholipids, Cardiolipin, Polar localisation, *Bacillus subtilis*

Abbreviations: NAO, 10-nonylacridine orange bromide; Nile Red, 9-diethylamino-5-benzo[α]phenoxazinone.

ABSTRACT

Rather than being a homogenous diffusion-dominated structure, biological membranes can exhibit areas with distinct composition and characteristics commonly termed as lipid domains. Arguably the most comprehensively studied examples in bacteria are domains formed by cardiolipin, which have been functionally linked to polar protein targeting, cell division process, and mode of action of membrane targeting antimicrobials. Cardiolipin domains were originally identified in the Gram-negative model organism *Escherichia coli* based on preferential staining by the fluorescent membrane dye nonyl acridine orange (NAO), and later reported to exist also in other Gram-negative and -positive bacteria. Recently, the lipid-specificity of NAO has been questioned based on studies conducted in *E. coli*. This prompted us to re-analyse cardiolipin domains also in the Gram-positive model organism *B. subtilis*. Here we show that logarithmically growing *B. subtilis* does not form detectable cardiolipin-specific lipid domains, and that NAO is not a specific stain for cardiolipin in this organism.

FULL-TEXT

Our understanding of the structure and organisation of biological membranes is based on the classical fluid mosaic model of Singer and Nicolson, which describes biological membranes as a homogeneous two-dimensional fluid dominated by free lateral diffusion of lipids and embedded proteins [1]. However, last decades of research have revealed that biological membranes are far more complex and heterogeneous than originally assumed, and specific lipid species can form distinct domains within biological membranes that fulfil specific biological functions [2, 3]. Arguably the most comprehensively studied type of bacterial lipid domain are clusters of cardiolipin forming at bacterial cell poles and cell division sites [4]. Cardiolipin is a complex phospholipid species commonly found in bacterial membranes, which is formed by two phosphatidylglycerol lipids linked together by an additional glycerol via phosphodiester bonds. Consequently, cardiolipin carries a double negative charge, a total of four fatty acid chains, and has an atypical conical molecular shape [5]. What makes cardiolipin unique in the context of lipid domain studies is the existence a cardiolipin-specific fluorescent membrane dye nonyl acridine orange (NAO) that allows the localisation and clustering-behaviour of cardiolipin to be analysed in living bacterial cells [4, 6]. Due to its positive charge, NAO preferentially stains membranes containing anionic phospholipids. Upon interaction with cardiolipin, NAO undergoes a redshift in the fluorescent emission spectrum, thereby allowing the microscopic identification and visualisation of membrane areas that are enriched in cardiolipin [4, 6].

By using NAO-staining, Mileykovskaya and co-workers showed in their seminal study that *E. coli* membranes contain specific cardiolipin-enriched lipid domains that are localised at the cell poles and cell division sites [6]. Importantly, these findings were independently confirmed by analysing the composition of so-called minicells. These small cells are formed by a misplaced cell division occurring at the cell pole, which results in small anucleate cells that are highly enriched in cell material normally found at the cell poles. The analysis of the lipid composition of minicells revealed a clear enrichment of cardiolipin, thereby providing strong support for the polar cardiolipin domain hypothesis [7]. The mechanism through which cardiolipin accumulates at the cell poles is linked to the atypical conical shape of the cardiolipin molecule, which provides preference to curved membrane found at the cell poles [8-10]. By forming a polar landmark that allows cardiolipin-interacting proteins to be specifically

targeted to bacterial cell poles, cardiolipin domains have been suggested to be functionally linked to several prominent cellular processes such as cell division, chemotaxis, and transport [11-15]. At last, due to the high negative surface charge, polar cardiolipin domains have been discussed as preferred targets for cationic membrane targeting antimicrobials such as host immunity peptides [16-19].

Recently, however, the strict specificity of NAO towards cardiolipin has been questioned [20]. By carefully analysing the staining-specificity both *in vitro* and *in vivo*, Oliver and co-workers concluded that the characteristic red-shifted fluorescence emission of NAO is not specific for dye molecules interacting with cardiolipin but rather promiscuous for anionic phospholipids in general. These studies were conducted in the Gram-negative model organism *E. coli* and much less attention has been given to other bacteria with respect to rigorous testing the specificity of NAO-staining. Instead, the broad conservation of cardiolipin-specific domains among bacterial species has been largely accepted within the community. Due to the concerns emerging from the *E. coli* studies, we decided to reanalyse both the existence of cardiolipin-domains, and the staining-specificity of NAO in the Gram-positive model organism *B. subtilis*.

To our surprise, when we stained *B. subtilis* wild type cells grown in LB medium with low concentrations of NAO (100 nM), we did not observe the previously reported lipid domains (Fig. 1a). Instead, the NOA membrane stain was perfectly smooth both in the green wavelength range (500-550 nm), and in the potentially cardiolipin-specific red wavelength range (593-667 nm). In both cases, the fluorophore was exited with 450-490 nm light. The only detectable local enrichment in fluorescent NAO-signal was the enhanced fluorescence emitted by the septum; a phenomenon originating from close proximity of two parallel membranes present at septum, which results in an increased septal signal of any disperse membrane-associated fluorophore. The same absence of detectable lipid domains was observed in DSM medium, which was the medium used in the original publication describing cardiolipin domains in *B. subtilis* (Fig. 1a) [21]. In our laboratory, the standard technique to stain cells with membrane dyes is to withdraw a 100-200 µl aliquot of an actively growing culture, and to stain the cell suspension in a round bottom 2 ml Eppendorf tube with a perforated lid at the growth temperature, and upon constant shaking. This is to ensure continuous aeration of the culture, which is crucial to maintain the cells adequately energised [22, 23], and to minimise changes in temperature,

which can directly influence the analysed membranes by altering membrane fluidity and by triggering adaptation of the lipid composition [24, 25]. While the exact staining conditions are not comprehensively described in the original publication, the authors do mention that the staining was carried out for 20 min at room temperature [21]. To test if different staining temperatures could explain the discrepancy, we repeated the experiments with staining taking place at 20°C, as opposed to incubation at the growth temperature of 37°C. Indeed, under these conditions we could reproduce the previously published staining pattern with distinct domains present in the cytoplasmic membranes (Figs. 1b and S1). However, a frequent domain formation was only observed in cells grown in the DSM medium. A large majority of cells grown in LB medium were free of NAO-stained lipid domains even upon staining at 20°C (Figs. 1b and S1). Consequently, we must conclude that actively growing *B. subtilis* cells do not form lipid domains than can be preferentially stained by NAO. Instead, the detected domains are a consequence of the staining procedure, and are limited to certain growth media.

Next, we analysed the cardiolipin-specificity of the staining pattern observed in DSM medium upon cold shock. For this aim, we used a strain that carries deletions of the three known cardiolipin synthase genes *clsA*, *clsB* and *ywiE*. To verify that our strain indeed does not synthesise cardiolipin, we compared the thin layer chromatography profiles of lipid extracts from both the wild type and the cardiolipin synthase-deficient strain. In brief, this analysis was carried out for cells grown in LB-medium at 37°C to an OD_{600} of 1.0 by extraction of polar lipids from freeze-dried cell pellet using a modified Bligh and Dyer-solvent extraction protocol (initial extraction in choroform:methanol:0.3% aqueous NaCl mixture of 1:2:0.8 (v/v/v), followed by transfer to the chloroform-phase by adjustment to a ratio of 1:1:0.9) [26]. The TLC analysis and the identification of individual phospholipid species were carried out as described in Tindall *et al.* (2007) [27]. The extraction and identification of the phospholipids was carried out by the Identification Service of the DSMZ, Braunschweig, Germany. As shown in Fig. 2a, the membranes of the tested cardiolipin synthase-deficient strain do not contain detectable levels of cardiolipin. Unexpectedly, the domain formation observed upon cold shock with NAO turned out to be indistinguishable between wild type cells and cardiolipin-deficient cells, thus arguing that the observed domains are not specific clusters of cardiolipin (Fig. 2a). The existence of NAO-stained polar lipid domains in the absence of cardiolipin have also been reported for *E. coli* [20].

In this case, the domain formation was shown to require the synthesis of another common anionic lipid species phosphatidylglycerol. Hence, clustering of other negatively charged phospholipids that accumulate at the cell poles in the absence of cardiolipin was put forward as an explanation for the observed domains [20]. In contrast to *E. coli*, phosphatidylglycerol is an essential phospholipid species in *B. subtilis*, and depletion of phosphatidylglycerol synthase PgsA results in a lethal loss of membrane integrity [28]. Therefore, we chose to test the anionic nature of the observed lipid domains with an alternative method, and repeated the membrane staining of the cardiolipin-deficient deletion mutant with an uncharged fluorescent membrane dye Nile Red [29, 30]. The cold shock-triggered lipid domain pattern was readily detectable also with Nile Red (Fig. 2b), thus ruling out a charge-driven mechanism for the preferential staining. While this experiment formally does not disprove the possibility that the observed domains are enriched in anionic phospholipids, negative charge appears not to be the defining feature of these domains. Thus, the cold-shock triggered domain formation in *B. subtilis* is most likely a phenomenon that is unrelated to the formation of polar anionic lipid domains in *E. coli*.

We have previously shown that dissipation of membrane potential results in delocalisation of bacterial actin homologs MreB, Mbl, and MreBH; a process that is linked to formation of fluid lipid domains that can be visualised with Nile Red [22, 28]. To test if the cold-shock induced lipid domains also depend on MreB-homologs, we repeated the membrane staining experiments in a strain that is deleted for *mreB*, *mbl*, and *mreBH*. However, these cells, which have lost their rod-shape due to the absence of MreB-dependent lateral cell wall synthesis [31], were still forming NAO and Nile Red stained lipid domains in a cold shock-dependent manner (Figs. 2b-c and S3). The mechanism that triggers the formation of the observed lipid domains upon cold shock, and the composition and physicochemical characteristic that define these domains remains elusive. More comprehensive future studies are needed to properly characterise this novel type of cold shock-triggered bacterial lipid domain. However, we must conclude that these lipid domains are not characterised by localised clustering of cardiolipin.

At last, throughout our experiments we did not observe a noticeable difference in the intensity of the fluorescence membrane staining between cells that synthesise cardiolipin and cells that do not. This was also true for the red wavelength range, which has been postulated to be specific for cardiolipin.

To quantify this, we measured the red fluorescence intensity profiles for 30 NAO-stained cells grown in LB medium for wild type (Fig. 2d) and for cardiolipin-deficient strain (Fig. 2e). These measurements clearly demonstrate that NAO-fluorescence is not a reliable reporter for cardiolipin in the Gram-positive model organism *B. subtilis*. In the wider context, these findings highlight that, rather than relying on data obtained from other species, the potential lipid-specificity of NAO must be verified for the used bacterial species on a case-by-case basis, by using appropriate lipid synthase deletion strains.

ACKNOWLEDGEMENT

We would like to acknowledge Kathi Scheinpflug for early microscopy experiments that led to this project.

FUNDING INFORMATION

Funding for this project was provided by Newcastle University.

CONFLICTS OF INTEREST

The authors declare that there are no conflicts of interest.

REFERENCES

1. **Singer SJ, Nicolson GL**. The fluid mosaic model of the structure of cell membranes. *Science* 1972;175:720-731.
2. **Nicolson GL**. The fluid-mosaic model of membrane structure: still relevant to understanding the structure, function and dynamics of biological membranes after more than 40 years. *Biochim Biophys Acta* 2014;1838:1451-1466.
3. **Vereb G, Szollosi J, Matko J, Nagy P, Farkas T et al.** Dynamic, yet structured: The cell membrane three decades after the Singer-Nicolson model. *Proc Natl Acad Sci U S A* 2003;100:8053-8058.
4. **Mileykovskaya E, Dowhan W**. Cardiolipin membrane domains in prokaryotes and eukaryotes. *Biochim Biophys Acta* 2009;1788:2084-2091.
5. **Huang KC, Ramamurthi KS**. Macromolecules that prefer their membranes curvy. *Mol Microbiol* 2010;76:822-832.
6. **Mileykovskaya E, Dowhan W**. Visualization of phospholipid domains in *Escherichia coli* by using the cardiolipin-specific fluorescent dye 10-N-nonyl acridine orange. *J Bacteriol* 2000;182:1172-1175.
7. **Koppelman CM, Den Blaauwen T, Duursma MC, Heeren RM, Nanninga N**. *Escherichia coli* minicell membranes are enriched in cardiolipin. *J Bacteriol* 2001;183:6144-6147.
8. **Huang KC, Mukhopadhyay R, Wingreen NS**. A curvature-mediated mechanism for localization of lipids to bacterial poles. *PLoS Comp Biol* 2006;2:e151.
9. **Mukhopadhyay R, Huang KC, Wingreen NS**. Lipid localization in bacterial cells through curvature-mediated microphase separation. *Biophys J* 2008;95:1034-1049.
10. **Renner LD, Weibel DB**. Cardiolipin microdomains localize to negatively curved regions of *Escherichia coli* membranes. *Proc Natl Acad Sci U S A* 2011;108:6264-6269.
11. **Shiomi D, Yoshimoto M, Homma M, Kawagishi I**. Helical distribution of the bacterial chemoreceptor via colocalization with the Sec protein translocation machinery. *Mol Microbiol* 2006;60:894-906.
12. **Romantsov T, Stalker L, Culham DE, Wood JM**. Cardiolipin controls the osmotic stress response and the subcellular location of transporter ProP in *Escherichia coli*. *J Biol Chem* 2008;283:12314-12323.
13. **Matsumoto K, Kusaka J, Nishibori A, Hara H**. Lipid domains in bacterial membranes. *Mol Microbiol* 2006;61:1110-1117.
14. **Nishibori A, Kusaka J, Hara H, Umeda M, Matsumoto K**. Phosphatidylethanolamine domains and localization of phospholipid synthases in *Bacillus subtilis* membranes. *J Bacteriol* 2005;187:2163-2174.
15. **Romantsov T, Battle AR, Hendel JL, Martinac B, Wood JM**. Protein localization in *Escherichia coli* cells: comparison of the cytoplasmic membrane proteins ProP, LacY, ProW, AqpZ, MscS, and MscL. *J Bacteriol* 2010;192:912-924.
16. **Tran TT, Panesso D, Mishra NN, Mileykovskaya E, Guan Z et al.** Daptomycin-resistant *Enterococcus faecalis* diverts the antibiotic molecule from the division septum and remodels cell membrane phospholipids. *MBio* 2013;4.
17. **Rashid R, Veleba M, Kline KA**. Focal targeting of the bacterial envelope by antimicrobial peptides. *Front Cell Dev Biol*, 2016;4.
18. **Epand RM, Epand RF**. Lipid domains in bacterial membranes and the action of antimicrobial agents. *Biochim Biophys Acta* 2009;1788:289-294.
19. **Malanovic N, Lohner K**. Antimicrobial peptides targeting Gram-positive bacteria. *Pharmaceuticals* 2016;9.
20. **Oliver PM, Crooks JA, Leidl M, Yoon EJ, Saghatelian A et al.** Localization of anionic phospholipids in *Escherichia coli* cells. *J Bacteriol* 2014;196:3386-3398.
21. **Kawai F, Shoda M, Harashima R, Sadaie Y, Hara H et al.** Cardiolipin domains in *Bacillus subtilis* Marburg membranes. *J Bacteriol* 2004;186:1475-1483.
22. **Strahl H, Hamoen LW**. Membrane potential is important for bacterial cell division. *Proc Natl Acad Sci U S A* 2010;107:12281-12286.

23. **Te Winkel JD, Gray DA, Seistrup KH, Hamoen LW, Strahl H**. Analysis of antimicrobial-triggered membrane depolarization using voltage sensitive dyes. *Front Cell Dev Biol* 2016;4:29.
24. **Hazel JR**. Thermal adaptation in biological membranes - is homeoviscous adaptation the explanation. *Annu Rev Physiol* 1995;57:19-42.
25. **Parsons JB, Rock CO**. Bacterial lipids: metabolism and membrane homeostasis. *Prog Lipid Res* 2013;52:249-276.
26. **Bligh EG, Dyer WJ**. A rapid method of total lipid extraction and purification. *Can J Biochem Physiol* 1959;37(8):911-917.
27. **Tindall BJ, Sikorski J, Smibert RA, Krieg NR**. Phenotypic characterization and the principles of comparative systematics. In: Reddy C, Beveridge T, Breznak J, Marzluf G, Schmidt T, Snyder L (eds), *Methods for General and Molecular Microbiology*, 3rd edn. American Society of Microbiology; 2007, pp 330–393.
28. **Strahl H, Bürmann F, Hamoen LW**. The actin homologue MreB organizes the bacterial cell membrane. *Nat Commun* 2014;5.
29. **Greenspan P, Fowler SD**. Spectrofluorometric studies of the lipid probe, nile red. *J Lipid Res* 1985;26:781-789.
30. **Kucherak OA, Oncul S, Darwich Z, Yushchenko DA, Arntz Y et al.** Switchable nile red-based probe for cholesterol and lipid order at the outer leaflet of biomembranes. *J Am Chem Soc* 2010;132:4907-4916.
31. **Schirner K, Errington J**. The cell wall regulator σI specifically suppresses the lethal phenotype of *mbl* mutants in *Bacillus subtilis*. *J Bacteriol* 2009;191:1404-1413.
32. **Barbe V, Cruveiller S, Kunst F, Lenoble P, Meurice G et al.** From a consortium sequence to a unified sequence: the *Bacillus subtilis* 168 reference genome a decade later. *Microbiology* 2009;155:1758-1775.
33. **Salzberg LI, Helmann JD**. Phenotypic and transcriptomic characterization of *Bacillus subtilis* mutants with grossly altered membrane composition. *J Bacteriol* 2008;190:7797-7807.

249 **Table 1: Strains used in this study**

Strain	Relevant Genotype	Source	Construction
B. subtilis 168	*trpC2* (wild type)	[32]	-
B. subtilis SDB206	*clsA(ywnE)::ery clsB(ywjE)::spc ywiE::neo*	[21]	-
B. subtilis HB5347	*clsA(ywnE)::tet*	[33]	-
B. subtilis ARK3	*clsA(ywnE)::tet clsB(ywjE)::spc ywiE::neo*	this study	transformation of *clsA::tet*, *clsB::spc,* and *ywiE::neo* into *B. subtilis* 168
B. subtilis 4277	Ω*neo*3427 Δ*mreB mbl::cat mreBH::erm rsgI::spc*	[31]	-
B. subtilis KS60	Ωneo3427 Δ*mreB mbl::cat mreBH::erm rsgI::spc*	this study	transformation of Ωneo3427 Δ*mreB, mbl::cat, mreBH::erm, and rsgI::spc* into *B. subtilis* 168

250

Figure 1

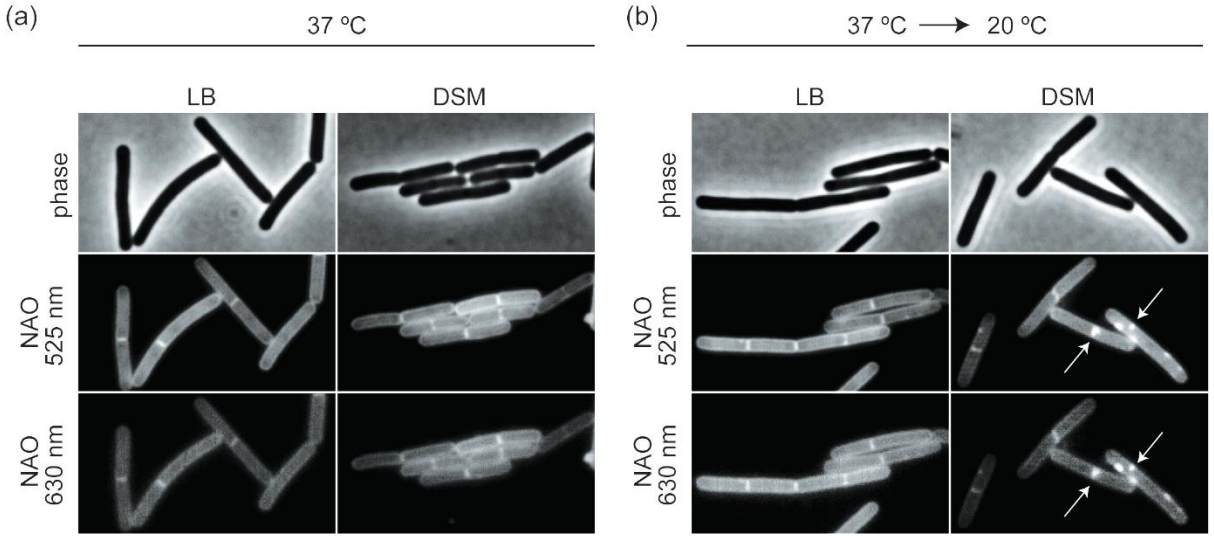

Fig. 1. (a) Phase-contrast images (upper panels), and NAO fluorescent membrane stains at 525 nm (middle panels) and at 630 nm (lower panels) of logarithmic growth phase *B. subtilis* cells grown in LB and DSM-media at 37°C, respectively. For these images the cells were stained for 20 min at 37 °C. (b) Comparable phase-contrast and fluorescent micrographs of *B. subtilis* cells grown at 37 °C, but stained with NAO for 20 min at 20°C. Few of the emerging domains are indicated with arrows. The final concentration of NAO upon staining was 100 nM. Strain used: *B. subtilis* 168 (wild type). See supplementary Fig. 1 for a larger field of view with more cells.

Figure 2

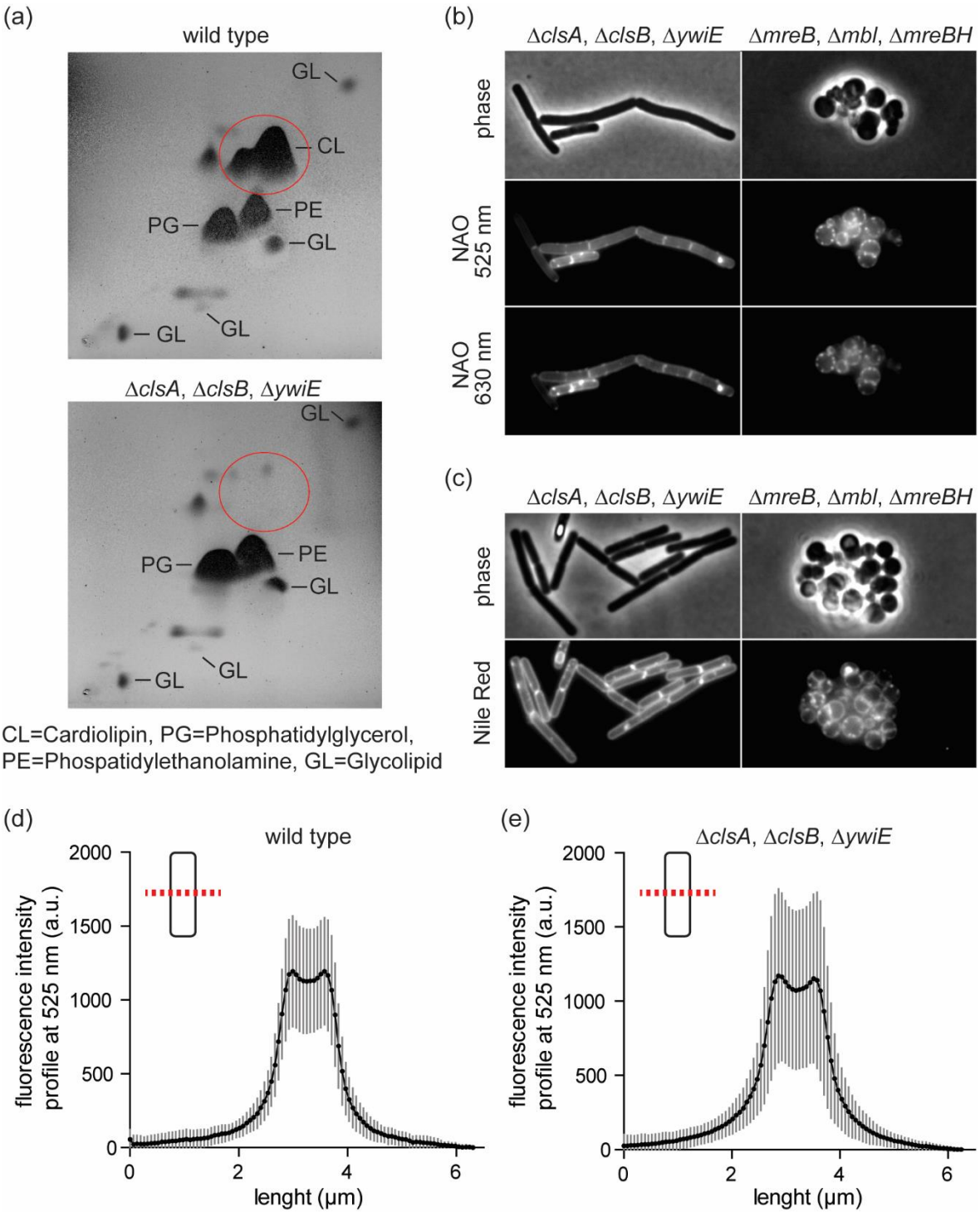

Fig. 2. (a) Thin layer chromatography showing the phospholipid profiles of *B. subtilis* wild type, and *B. subtilis* strain deficient for cardiolipin synthase homologs. For the TLC-analysis, the cells were grown in LB medium at 37 °C, and harvested at OD_{600}=1.0. (b) Phase-contrast images (upper panels), and NAO fluorescent membrane stains at 525 nm (middle panels) and at 630 nm (lower panels) of

logarithmic growth phase *B. subtilis* cells deficient for cardiolipin synthase homologs (left panels) and MreB homologs (right panels). The final concentration of NAO upon staining was 100 nM. (c) Phase-contrast images (upper panels), and Nile Red fluorescent membrane stains (lower panels) of logarithmic growth phase *B. subtilis* cells deficient for cardiolipin synthase homologs (left panels) and MreB homologs (right panels). The final concentration of Nile Red upon staining was 500 nM. The cells shown in panels (b) and (c) were grown in DSM medium at 37 °C, followed by staining for 20 min at 20 °C. In case of Nile Red, the dye was added only for the last 5 min of the 20 °C incubation period. The *mreB*-triple deletion mutant was grown in DSM medium supplemented with 20 mM $MgCl_2$, which is required for the growth of this strain. See Fig. S2 and S3 for comparable micrographs of cells stained at the growth temperature (37 °C). (d/e) NAO fluorescence intensity profiles measured perpendicular to the cell length axis for *B. subtilis* wildtype cells (d), and for cells deficient for cardiolipin synthase homologs (e). Both graphs depict the average and standard deviations of profiles from 30 individual cells. Strains used: *B. subtilis* 168 (wild type), *B. subtilis* ARK3 (deficient for cardiolipin), and *B. subtilis* KS60 (deficient for MreB-homologs).

Supplementary Information

Figure S1

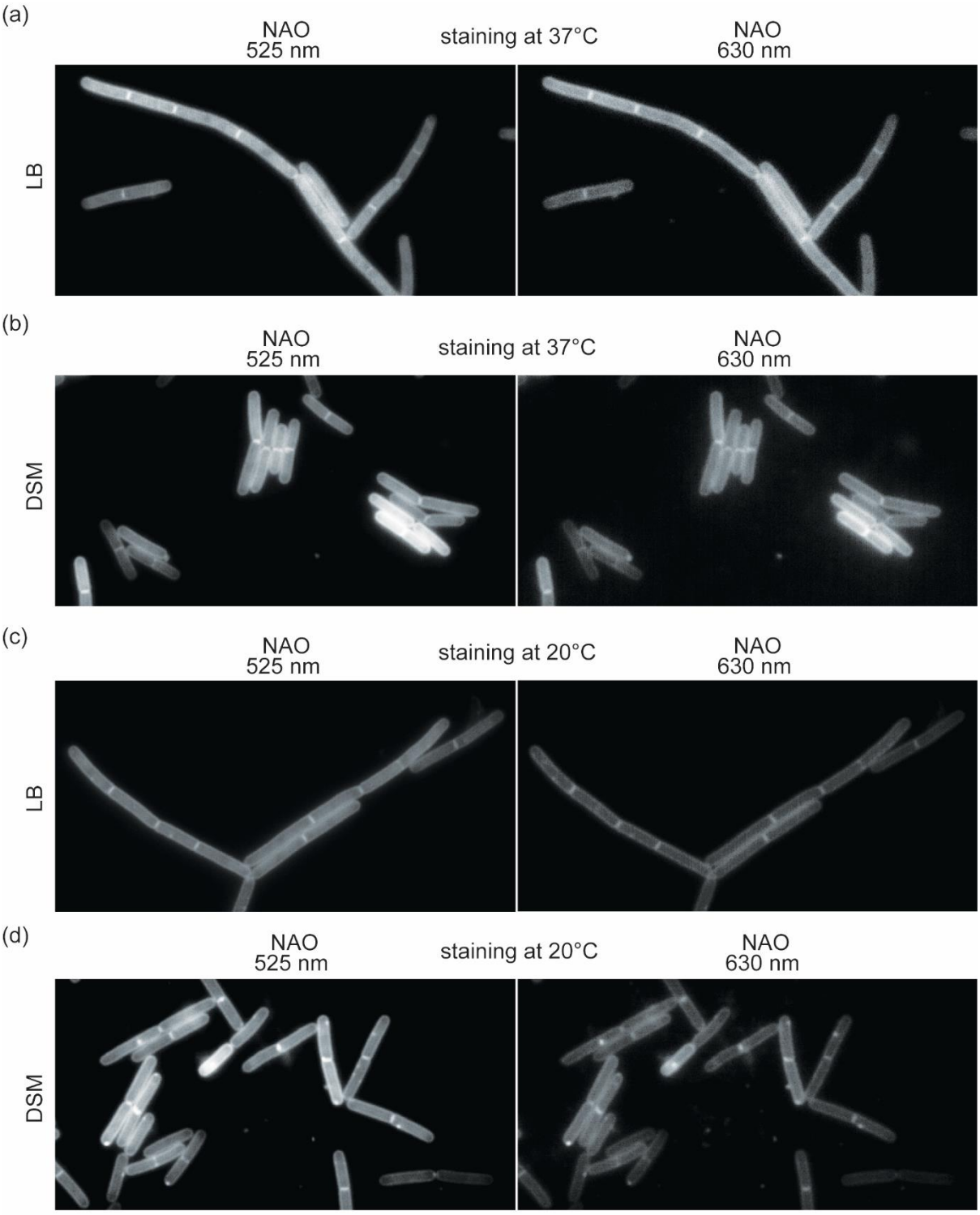

Fig. S1. NAO fluorescent membrane stains at 525 nm (left panels) and at 630 nm (right panels) of logarithmic growth phase *B. subtilis* cells grown in LB (a) and DSM (b) media at 37°C, respectively.

For these images, the cells were stained for 20 min at 37 °C. Comparable fluorescent micrographs of logarithmic growth phase *B. subtilis* cells grown at 37 °C in LB (c) and DSM-media (d), but stained with NAO for 20 min at 20°C. Note that the visible domains are absent in all fields except those shown in panel d. Strain used: *B. subtilis* 168 wildtype. This is a larger field of view of cells shown in Fig. 1. Strain used: *B. subtilis* 168 (wildtype).

Figure S2

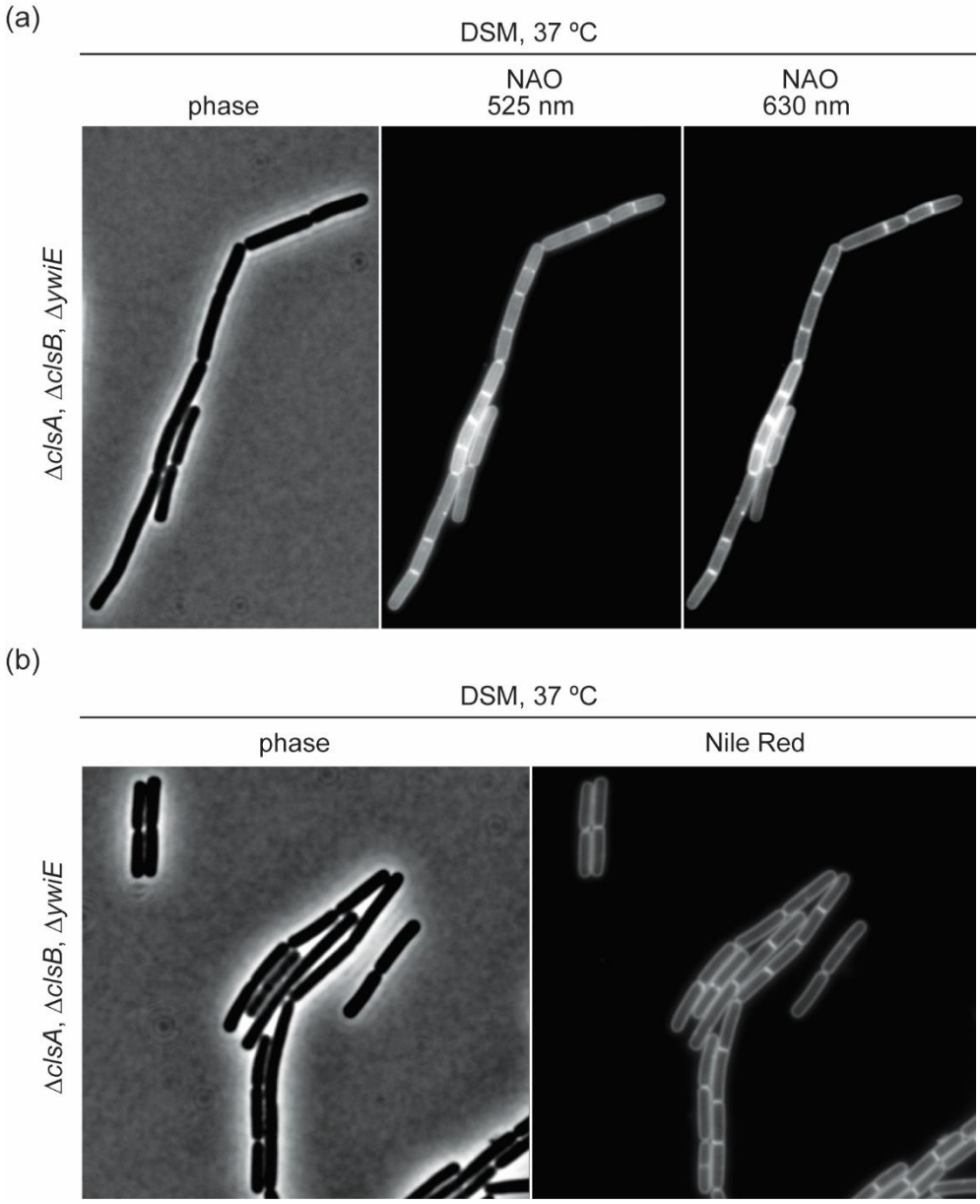

Fig. S2. (a) Phase-contrast images (left panel), and NAO fluorescent membrane stains at 525 nm (middle panel) and at 630 nm (right panels) of logarithmic growth phase *B. subtilis* cells deficient for cardiolipin synthases. (b) Phase-contrast images (left panel) and Nile Red fluorescent membrane stains (right panel) of logarithmic growth phase *B. subtilis* cells deficient for cardiolipin synthases. For these micrographs the cells were grown in DSM medium, and stained with NAO for 20 min at the growth temperature (37°C). Note that visible domains are absent in all shown fields. Strain used: *B. subtilis* ARK3 (deficient for cardiolipin).

Figure S3

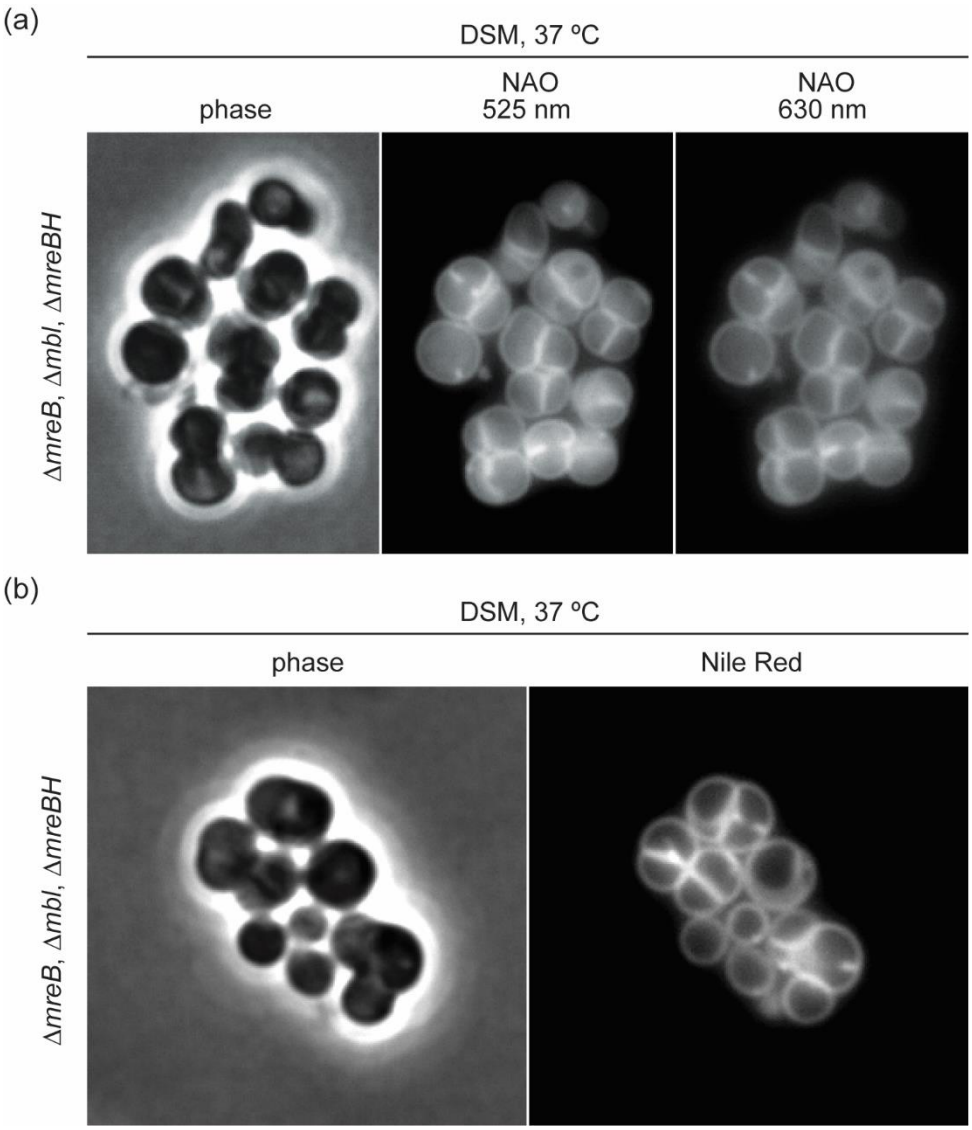

Fig. S3. (a) Phase-contrast images (left panel), and NAO fluorescent membrane stains at 525 nm (middle panel) and at 630 nm (right panels) of logarithmic growth phase *B. subtilis* cells deficient for MreB-homologs. (b) Phase-contrast images (left panel) and Nile Red fluorescent membrane stains (right panel) of logarithmic growth phase *B. subtilis* cells deficient for MreB-homologs. For these micrographs the cells were grown in DSM medium, and stained with NAO for 20 min at the growth temperature (37°C). Note that visible domains are absent in all shown fields. Strain used: *B. subtilis* KS60 (deficient for MreB-homologs).